This work was supported in part by a grant from the ERP fund.

References

ALBRECHT, W. W. & NIEDRIG, H. (1967). *Phys. Letters*, **26**A, 14.

ALBRECHT, W. W. & NIEDRIG, H. (1968). *J. Appl. Phys.* **39**, 3166.

BETHE, H. (1928). *Ann. Physik*, **87**, 55.

BOERSCH, H. (1947). *Z. Naturforschung*, **2a**, 615.

BOERSCH, H. (1948). *Optik*, **3**, 24.

BOERSCH, H., BOSTANJOGLO, O. & NIEDRIG, H. (1964). *Z. Physik*, **180**, 407.

BOERSCH, H., JESCHKE, G & RAITH, H. (1964). *Z. Physik*, **181**,436.

BOERSCH, H., JESCHKE, G. & WILLASCH, D. (1969). *Phys. Letters*. **29**A, 493.

BOERSCH, H., JUST, T. & NIEDRIG, H. (1969). *Phys. Letters*, **28**A, 709.

BOSTANJOGLO, O. & NIEDRIG, H. (1964). *Phys. Letters*, **13**, 23.

COWLEY, J. M. (1969). Private communication.

COWLEY, J. M. & MOODIE, A. F. (1957). *Acta Cryst.* **10**, 609.

COWLEY, J. M. & MOODIE, A. F. (1970). *Acta Cryst.* A**25**, 152.

COWLEY, J. M. & MURRAY, R. J. (1968). *Acta Cryst.* A**24**, 329.

DEBYE, P. (1914). *Ann. Physik*, **43**, 49.

DUPOUY, G., PERRIER, F., UYEDA, R., AYROLES, R. & MAZEL, A. (1965). *J. Microscopie*, **4**, 429.

FEENBERG, J. (1932). *Phys. Rev.* **40**, 40.

FUKUHARA, A. (1965). *Proc. Phys. Soc.* **86**, 1031.

GJØNNES, J. (1962). *Acta Cryst.* **15**, 703.

GLAESER, W. & NIEDRIG, H. (1966). *J. Appl. Phys.* **37**, 4303.

GLAUBER, R. & SCHOMAKER, V. (1953). *Phys. Rev.* **89**, 667.

GOODMAN, P. (1968). *Acta Cryst.* A**24**, 400.

GORINGE, M. J. (1966). *Phil. Mag.* **14**, 93.

HALL, C. R. & HIRSCH, P. B. (1965*a*). *Proc. Roy. Soc.* A**286**, 158.

HALL, C. R. & HIRSCH, P. B. (1965*b*). *Phil. Mag.* **12**, 539.

HOERNI, J. A. & IBERS, J. A. (1954). *Acta Cryst.* **7**, 405.

HOWIE, A. & WHELAN, M. J. (1961). *Proc. Roy. Soc.* A**263**, 217.

JESCHKE, G., RAITH, H. & ZORN, K. L. (1966). *Sixth Int. Conf. Electron Microscopy*, Kyoto, **1**, 97.

JESCHKE, G., NIEDRIG, H. & RIDDER, H. W. (1968). *Phys. Letters*, **28**A, 337.

KAINUMA, Y. & YOSHIOKA, H. (1966). *J. Phys. Soc. Japan*, **21**, 1352.

MEYER, G. (1966). *Phys. Letters*, **20**, 240.

MEYER-EHMSEN, G. (1969). *Z. Physik*, **218**, 352.

MOLIÈRE, K. (1939). *Ann. Physik*, **34**, 461.

OHTSUKI, Y. H. (1966). *J. Phys. Soc. Japan*, **21**, 2300.

RAITH, H. (1968). *Acta Cryst.* A**24**, 85.

SEVELY, J. (1969). Ph. D. Thesis, Toulouse.

UYEDA, R. (1968). IV*th Europ. Reg. Conf. Electron Microscopy*, Rome, **1**, 55.

VINGSBO, O. (1966). *Sixth Int. Conf. Electron Microscopy*, Kyoto, **1**, 109.

WATANABE, H. (1965). *Japan. J. Appl. Phys.* **4**, 384.

WHELAN, M. J. (1965). *J. Appl. Phys.* **36**, 2099.

YOSHIOKA, H. (1957). *J. Phys. Soc. Japan*, **12**, 618.

YOSHIOKA, H. & KAINUMA, Y. (1962). *J. Phys. Soc. Japan*, **17**, Suppl. B. II., 134.

Acta Cryst. (1970). A**26**, 118

Lorentz and Orientation Factors in Fiber X-ray Diffraction Analysis

BY R. J. CELLA, BYUNGKOOK LEE* AND R. E. HUGHES

Department of Chemistry, Cornell University, Ithaca, New York 14850, *U.S.A.*

(*Received* 1 *April* 1969)

The application of a general formulation of the Lorentz factor for any distribution of crystallite orientations to a uniaxial fiber structure reveals that current practice, which involves the use of a standard single-crystal rotation factor, is inadequate. An analysis is presented which eliminates the need for a detailed knowledge of the distribution function and which can be applied to measured peak intensities. The resulting expressions significantly improved the agreement between sets of experimental test data.

The Lorentz factor is applied to X-ray diffraction intensity data to account for the fact that not all sets of crystal planes have the same opportunity to diffract the incident beam. The form the factor takes depends not only on the kinematics of the diffraction system but also upon the nature of the crystalline sample. For single-crystal rotation techniques this geometric factor is a measure of the relative amount of time different sets of planes spend in the diffraction position or, alternatively, the relative amounts of time the corresponding reciprocal lattice points take in passing through the Ewald sphere. For stationary powder methods, it is simply the fractional number of reciprocal lattice points which lie on the surface of the Ewald sphere.

* Present address: Department of Molecular Biology and Biophysics, Yale University, New Haven, Connecticut 06520, U.S.A.

Previous workers have recognized (Franklin & Gosling, 1953; Arnott, 1965) that the standard correction factors are inadequate when applied to partially oriented macromolecular structures. Nevertheless, it is a fact that the single-crystal rotation factor is typically applied to the data from such systems. The present analysis provides a formalism for deriving the Lorentz factor for any geometric distribution of crystallites in a polycrystalline sample. In particular, it is applied to the uniaxial orientation characteristic of fibrous macromolecules.

The general Lorentz factor

It is required to derive a general expression for the Lorentz factor in terms of a distribution function characterizing crystallite orientations. An X-ray beam impinges upon a fiber tilted through an angle μ with respect to a plane normal to the beam; the sample is considered to be composed of a large number of well ordered crystallites with orientations given by $\Omega(\varrho, \theta)$. In a given crystallite, ϱ is the angle between the fiber axis and the unit normal, $\hat{\mathbf{n}}$, to the plane *hkl*. The density function, $\Omega(\varrho, \theta)$, can then be defined as the fractional number of unit normals, $\hat{\mathbf{n}}$, which lie in the unit solid angle at (ϱ, θ), where θ is one-half the angle between the incident beam and the diffracted beam (the scattering angle). For a given orientation, the intensity of radiation, I_S, scattered into a detector of area S from an incident beam, I_0, by a set of p parallel planes a distance t apart (Fig. 1), is given by:

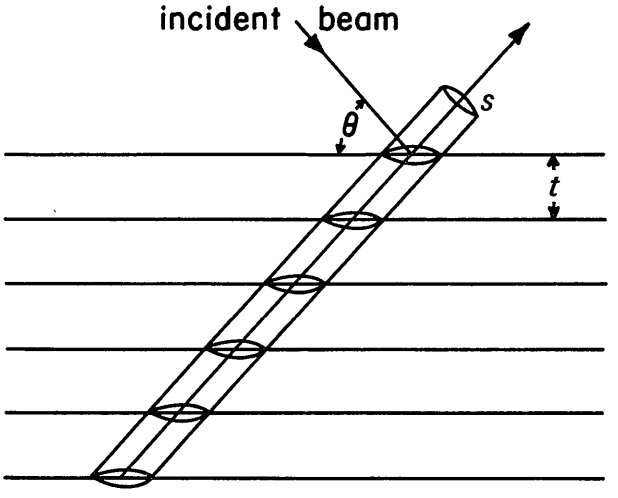

Fig. 1. Scattering from a set of uniformly spaced parallel planes.

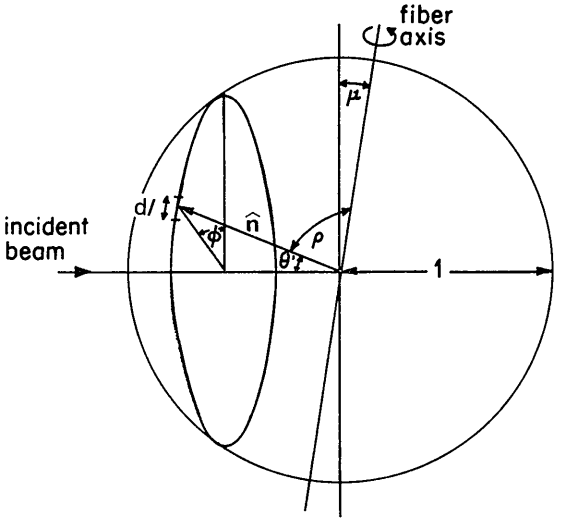

Fig. 2. Perspective diagram showing integration variables for calculation of general Lorentz factor; dl is the line element along the intersection of the cone of half angle θ' with a unit sphere.

$$I_S = I_0 R(\varepsilon)\,, \tag{1}$$

where

$$R(\varepsilon) = |F|^2 \left(\frac{N\lambda t}{\sin\theta}\right)^2 \left(\frac{e^2}{mc^2}\right)^2 \frac{\sin^2(pB\varepsilon)}{\sin^2(B\varepsilon)}$$

and

$$B = 2\pi t \cos\theta_0/\lambda\,.$$

In these expressions, $\varepsilon = \theta - \theta_0$ is the deviation of the scattering angle from the Bragg angle, θ_0, and the symbols F, N, λ, e, c, and m have their usual meanings (James, 1962).

The total energy, E, scattered into S by a given family of planes can be calculated by integrating the diffracted intensity, I_S, from all crystallites over all scattering angles. This can be expressed as

$$E = SI_0 \int\int R(\varepsilon)\Omega(\varrho, \theta)\mathrm{d}l\mathrm{d}\theta'\,, \tag{2}$$

where the contributions from individual crystallites are weighted by the orientation distribution function $\Omega(\varrho, \theta)$; the integration variable θ' is simply the complement of θ and l is defined in Fig. 2.

Through a rather tedious transformation, the integral can be expressed as a function of ϱ and θ, the variables of interest. In this form,

$$E = 2SI_0 \int\int R(\varepsilon)\Omega(\varrho, \theta)\Psi(\varrho, \theta)\cos\theta \sin\varrho\, \mathrm{d}\varrho\mathrm{d}\theta\,, \tag{3}$$

where

$$\Psi(\varrho, \theta) = [\cos^2\theta\cos^2\mu - (\cos\varrho + \sin\theta\sin\mu)^2]^{-\frac{1}{2}}\,.$$

Because the integrand contains the classical interference function in $R(\varepsilon)$, the integration over ε can be effected through standard formalisms after the appropriate transformation of variables. In the resulting expression,

$$E = I_0 N^2\lambda^3 \left(\frac{e^2}{mc^2}\right)^2 |F|^2 S \frac{pt}{\sin^2\theta} \times \int \Omega(\varrho, \theta)\Psi(\varrho, \theta)\sin\varrho\,\mathrm{d}\varrho\,, \tag{4}$$

it is now convenient to omit the subscript on the symbol for the Bragg angle. From Fig. 1 it is evident that $Spt/\sin\theta$ is the volume of the cylindrical element scattering into S. Calling this volume element dv and writing in the usual polarization factor, $p=\frac{1}{2}(1+\cos^2 2\theta)$, to allow for unpolarized X-rays, the integrated intensity becomes

$$E=I_0N^2\lambda^3\left(\frac{e^2}{mc^2}\right)^2|F|^2\frac{p\,dv}{\sin\theta}\times\int_{f_1(\mu,\theta)}^{f_2(\mu,\theta)}\Omega(\varrho,\theta)\Psi(\varrho,\theta)\sin\varrho\,d\varrho\,, \quad (5)$$

range in ϱ. Fig. 3 illustrates a distribution of unit normals, $\hat{\mathbf{n}}$, over an angular range of $2\Delta\varrho$ centered about ϱ_0, with a unit-normal density of zero outside this range. Rotation of this arc implies that $\Omega(\varrho,\theta)$ is independent of θ and is inversely proportional to the solid angle swept out by the spherical arc segment of height $2\sin\varrho_0\sin\Delta\varrho$. Thus, for a uniform distribution along ϱ,

$$\Omega(\varrho,\theta)=(4\pi\sin\varrho_0\sin\Delta\varrho)^{-1} \quad (8)$$

and, after integration in (6) between the limits $\varrho_0-\Delta\varrho$ and $\varrho_0+\Delta\varrho$, the Lorentz factor becomes

$$L=\frac{\left\{\sin^{-1}\left[\frac{\cos(\varrho_0-\Delta\varrho)}{\cos\theta\cos\mu}+\tan\theta\tan\mu\right]-\sin^{-1}\left[\frac{\cos(\varrho_0+\Delta\varrho)}{\cos\theta\cos\mu}+\tan\theta\tan\mu\right]\right\}}{4\pi\sin\theta\sin\varrho_0\sin\Delta\varrho}\,. \quad (9)$$

where the limits on the integration depend on the diffraction geometry. The Lorentz factor, L, can be drawn from the angular dependent terms of the preceding expression and is defined as

$$L=\frac{1}{\sin\theta}\int_{f_1(\mu,\theta)}^{f_2(\mu,\theta)}\Omega(\varrho,\theta)\Psi(\varrho,\theta)\sin\varrho\,d\varrho\,. \quad (6)$$

This is the desired formulation of the Lorentz factor in terms of a generalized distribution function and convenient integration variables. Before introducing the distribution function for fiber structures it will be shown that this general expression for L yields the correct results for several well known cases.

Random distribution

In the case of randomly oriented crystallites, as would be found in a powder sample, the unit normals are uniformly distributed, and the distribution function is independent of ϱ and θ. Thus, $\Omega(\varrho,\theta)$ is simply equal to $1/(4\pi)$, the fractional number of unit normals per unit solid angle. It can readily be seen from Fig. 2 that the appropriate integration limits are $f_1(\mu,\theta)=\theta+\mu$ and $f_2(\mu,\theta)=\pi-\theta+\mu$, whence the Lorentz factor becomes:

$$L=\frac{1}{\sin\theta}\int_{\theta+\mu}^{\pi-\theta+\mu}\frac{1}{4\pi}\Psi(\varrho,\theta)\sin\varrho\,d\varrho\,. \quad (7)$$

Inserting the expression for $\Psi(\varrho,\theta)$ from equation (3) and performing the integration, one obtains $L=(4\sin\theta)^{-1}$, which is the well established Lorentz factor for powder samples.

Single-crystal factors

It is convenient to develop the expressions for single-crystal rotation factors from slightly more general forms based upon the rotation of reciprocal lattice vectors which are distributed over a small angular

This expression can be specialized to the case of a single crystal by taking the limit as $\Delta\varrho\to 0$, whence the distribution function corresponds to that for a rotating single crystal. This yields the equation

$$L^{rot}=\lim_{\Delta\varrho\to 0}L=\frac{1}{2\pi\sin\theta}\Psi(\varrho,\theta) \quad (10)$$

which can be cast into more familiar forms by the following elementary transformations (Buerger, 1960):

$$4\sin^2\theta=\xi^2+(\sin\upsilon-\sin\mu)^2$$

$$\cos\varrho=\frac{\sin\upsilon-\sin\mu}{2\sin\theta}$$

$$\sin\varrho=\frac{\xi}{2\sin\theta}$$

in which υ is the angle between the generator of the nth layer line and the equatorial plane and ξ is the radial Bernal coordinate. The resulting expression,

$$L^{rot}=[(\xi+\cos\mu+\cos\upsilon)(-\xi+\cos\mu+\cos\upsilon)(\xi-\cos\mu+\cos\upsilon)(\xi+\cos\mu-\cos\upsilon)]^{-\frac{1}{2}}\,, \quad (11)$$

is the established Lorentz factor for the general inclination method. The normal-beam rotation factor is a special case of (11) with $\mu=0$, and the zero level rotation factor involves the further specialization, $\mu=\upsilon$.

Fiber orientation – a geometric approach

An oriented macromolecular fiber can be described in terms of an axially symmetric function which characterizes the azimuthal distribution of crystallite orientations with respect to the fiber axis. In reciprocal space, this corresponds to a distribution of reciprocal lattice points on circular bands generated by the rotation around the fiber axis of spherical arc segments of angle $2\Delta\varrho$. The intersection of such a circular band

with the Ewald sphere is shown in Fig. 3; the distribution of reciprocal lattice points along the arc of intersection depends upon $\Omega(\varrho, \theta)$. The actual distribution function along ϱ for a given system would be difficult to determine; one might suppose that a Gaussian function would provide a good approximation. Dependence upon θ would imply biaxial orientation and will not be considered here. For present purposes, it will be shown that the Lorentz factor corresponding to a hypothetical rectangular distribution along ϱ can be calculated from simple geometric arguments in reciprocal space. In a later section it will be shown that the need for an exact knowledge of the distribution function can be avoided in a more general treatment.

The Lorentz factor is proportional to the ratio of the length of the arc which is the locus of the intersection of the circular band with the Ewald sphere to the area of the circular band itself, the latter being multiplied by $\cos\theta$ to account for the finite thickness of the band and its oblique intersection with the sphere. A reasonably straightforward geometric calculation shows the arc length to be

$$s=2\sin 2\theta\left\{\sin^{-1}\left[\frac{\cos(\varrho_0-\Delta\varrho)}{\cos\theta\cos\mu}+\tan\theta\tan\mu\right]-\sin^{-1}\left[\frac{\cos(\varrho_0+\Delta\varrho)}{\cos\theta\cos\mu}+\tan\theta\tan\mu\right]\right\}, \quad (12)$$

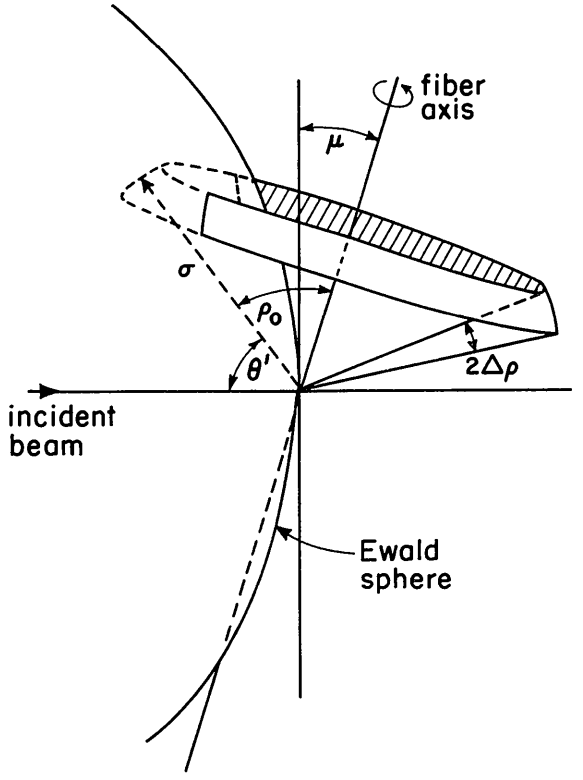

Fig. 3. Intersection of a circular band of reciprocal lattice points with the Ewald sphere.

and the area of the circular band is $4\pi\sigma^2\sin\varrho_0\sin\Delta\varrho$, where $\sigma=2\sin\theta$ is the length of the reciprocal lattice vector. The ratio of these two quantities yields an expression for the Lorentz factor which is identical to equation (9) which was derived from the general integral formulation of L given in (6).

This geometric approach is the one used by Arnott (1965) in his treatment of the problem. It should be noted that his expression for the arc length contains a slight error in the terms involving $\tan\theta$ in (12); however his final expression for L was unaffected by this error. Of greater importance is the fact, unnoted in his report, that by taking the limit of L as $\Delta\varrho\to 0$ he simply derived a form of equation (11), the single-crystal rotation Lorentz factor. This fact was masked by the somewhat unusual form of his result but it can readily be demonstrated by appropriate substitutions.* Thus, it is clear that a more complete analysis of the problem based upon the generalized formulation of the Lorentz factor given in equation (6) is required.

The use of peak intensities

Evaluation of the desired quantities, $|F|$, from equation (5) requires, in addition to a set of integrated intensities, a knowledge of the distribution function $\Omega(\varrho, \theta)$. Integrated intensities are difficult to measure along the ill-defined arcs of variable length and the Lorentz factor associated with each element along the arc changes continuously. The distribution function could be deduced from the intensity variation along the arcs but only through an extensive series of careful measurements. It clearly would be of considerable value to be able to calculate corrected values of $|F|$ from measurements of the peak intensities at the centers of the arcs; the following analysis shows that this can be done.

The arc length on the Ewald sphere associated with a given reflection with an axially symmetric fiber distribution function of angular range $2\Delta\varrho$ is given by equation (12). The projected length of this arc from the center of the sphere depends upon the geometry of the recording system. For a cylindrical film and normal beam incidence, each arc is centered at ϱ_0 and extends $\pm\Delta\varrho$ along lines of constant θ; the variation in length of such an arc across a film can readily be seen in the $\varrho-\theta$ chart in Fig. 4. Since the apparent angular spread of the arc will depend upon the time of exposure it is necessary to relate the structure factor to an intensity measurement taken over a finite range at ϱ_0.

For a non-uniform distribution, equation (8) can be rewritten

$$\Omega(\varrho)=(4\pi\sin\varrho_0\sin\Delta\varrho)^{-1}n(\varrho-\varrho_0), \quad (13)$$

where the function $n(\varrho-\varrho_0)$ describes the distribution

* It should be noted that ϱ and σ in the present manuscript correspond to the symbols θ and ϱ, respectively, in Arnott (1965).

of unit normals along ϱ in the circular band. This distribution can be divided into smaller bands of angular spread $2\delta\varrho$ with $\delta\varrho \ll \Delta\varrho$, each centered about ϱ_i as shown in Fig. 5. Then,

$$\Omega_i(\varrho) = (4\pi \sin \varrho_i \sin \delta\varrho)^{-1} n_i(\varrho - \varrho_i) , \qquad (14)$$

and the integrated intensity can be expressed as a sum of terms, each of the form of equation (5) and each containing $\Omega_i(\varrho)$ from (14).

If $\delta\varrho$ is sufficiently small, it may be assumed that $n_i(\varrho - \varrho_i)$ is a constant and, if the measurement is made around ϱ_0 at the center of the band, the Lorentz factor is proportional to the expression in (9). Moreover, if $\delta\varrho$ is sufficiently small, the limiting process in which $\delta\varrho \to 0$ can be neglected so that the integrated intensity in this angular range at ϱ_0 becomes

$$I_{\varrho_0} = K|F|^2 p n(\varrho - \varrho_0) \mathrm{L}^{\mathrm{rot}}(\varrho_0) . \qquad (15)$$

In this expression $\mathrm{L}^{\mathrm{rot}}(\varrho_0)$ is the usual rotation factor of equation (10) evaluated at ϱ_0 and $n(\varrho - \varrho_0)$ is a constant for all reflections as long as intensity measurements are made at corresponding points (such as ϱ_0) along the distribution functions. The constant K is the collection of constants in equation (5).

Thus, it appears that single-crystal rotation factors can be applied to measured intensity data, but it must be emphasized that equation (15) applies *only* to measurements made over a constant angular range, $\delta\varrho$. This means that a variable length of each reflection must be measured or, alternatively, appropriate correc-

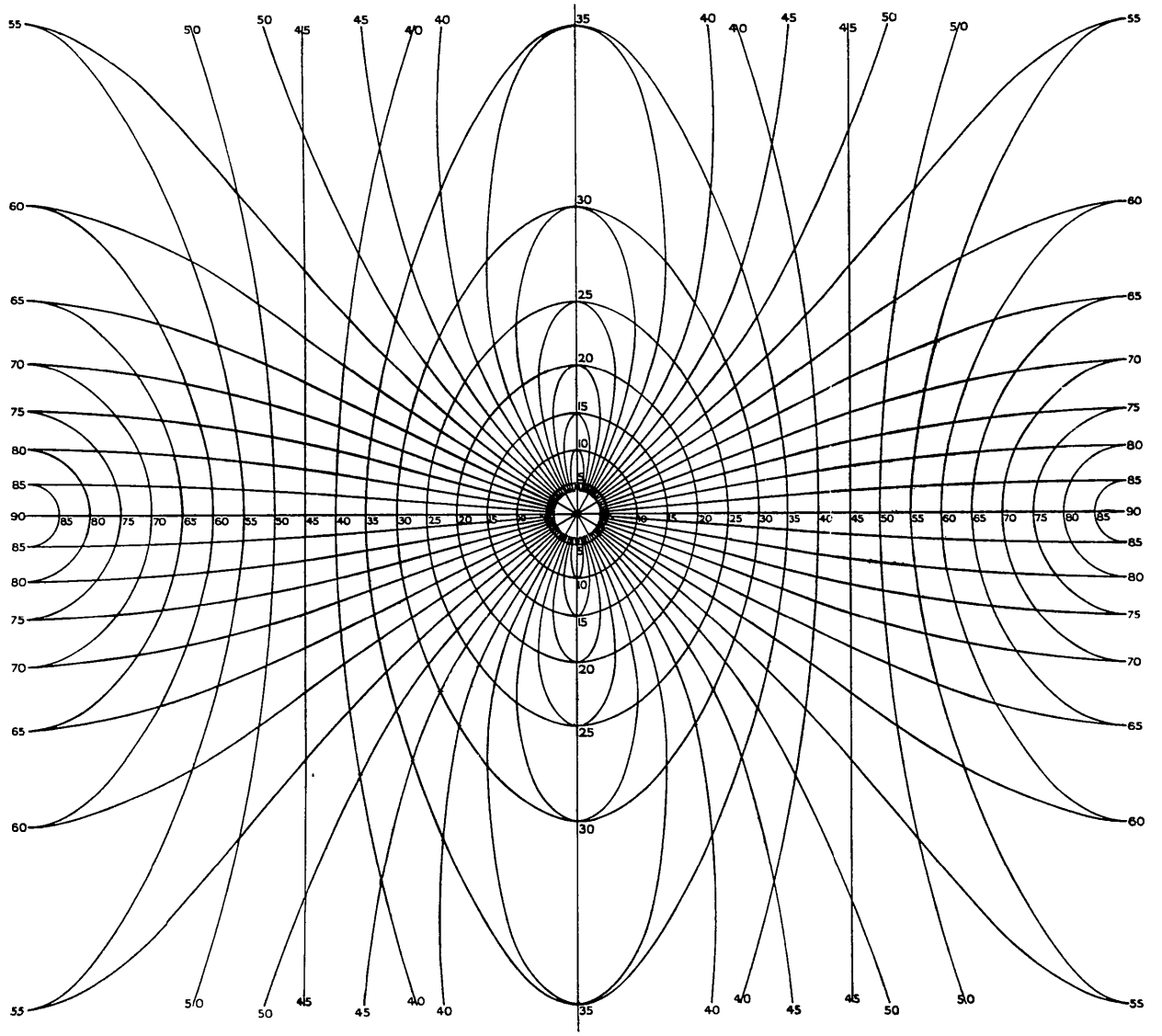

Fig. 4. Lines of constant ϱ and constant θ over the surface of a cylindrical film.

tion factors must be applied; the latter are developed in the following section.

Arc correction factors

If intensities are measured by traversing a section of each arc with a detector of fixed slit width, such as a microdensitometer or a scintillation counter, the angular range actually recorded will differ for each reflection and will depend upon the direction of traversal and upon the diffraction geometry. Moreover, since the total length of each arc is indeterminate, the correction factor which scales all arcs to the same angular range can only be determined on a relative basis. The arc *length* on the film (or at the counter) which corresponds to a given $\Delta\varrho$ can be calculated using equation (12) and standard transformations relating film coordinates to reciprocal lattice coordinates (Buerger, 1942). From such expressions, arc correction factors can be defined which are inversely proportional (in the limit as $\Delta\varrho \to \delta\varrho \to 0$) to the angular spread in ϱ actually encompassed at each reflection by the small, fixed slit width. This turns out to be a surprisingly awkward procedure and yields complex transcendental expressions which are useful only in numerical analyses on a computer. The problem can be linearized to a very good approximation by using, instead, the limiting ratios of a simple function of arc chords. The results from such an analysis are summarized below in terms of reciprocal space coordinates for a number of experimental situations.

For normal-beam techniques, the structure factors are related to the peak intensities, integrated in the direction of scan, I_{ϱ_0}, by

$$|F|^2 = \frac{k\Gamma I_{\varrho_0}}{\mathrm{Lp}} \tag{16}$$

where k is a collection of constants which becomes a scale factor and L is the single-crystal rotation Lorentz factor. For cylindrical films, Γ, the orientation correction factor, is given by

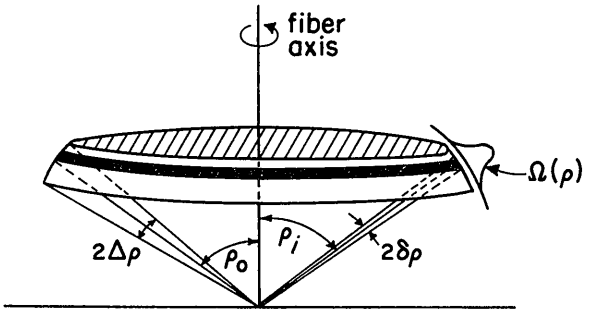

Fig. 5. Subdivision of the circular band of angular range $2\Delta\varrho$ into sub-bands of angular range $2\delta\varrho$. The distribution function $\Omega(\varrho,\theta)$ is decomposed into the functions $n(\varrho-\varrho_i)$ over $2\delta\varrho_i$.

$$\Gamma = \frac{\xi}{(1-\zeta^2)^{3/2}}\left[1+\frac{\zeta^2}{4}\left(\frac{1}{(2-\sigma^2)^2}-\frac{1}{1-\zeta^2}\right)\right]^{m/2} \tag{17}$$

and for flat films, it is

$$\Gamma = \frac{\xi}{2-\sigma^2}\left[1-\frac{4\zeta^2}{4\sigma^2-\sigma^4}\right]^{-m/2}. \tag{18}$$

In these expressions, $m=0$ if the peak intensity is integrated along a path which is perpendicular to the fiber axis and $m=1$ if the path is perpendicular to the arc at ϱ_0 (as would be true, for example, with a radial tracing on a flat film).

For intensities that are measured by visual comparison with a standardized series of reference arcs, these correction factors are applicable with $m=1$ if (i) the reference arcs are placed parallel to the reflection arcs and (ii) if the intensities are compared at ϱ_0 through a slit perpendicular to the arcs.

It must be emphasized that the preceding analyses are applicable only to normal beam techniques. While additional data are often accessible by tilting the fiber, the correction factors become exceedingly complex and such data must be used cautiously, if at all, in structure refinement.

An experimental test

Diffraction data were obtained from a moderately well oriented polyethylene fiber with normal beam incidence in a cylindrical camera of 57·3 mm diameter. Three sets of photographs were taken with Co $K\alpha$, Cu $K\alpha$ and Cr $K\alpha$ radiation; this ensured that each reflection required a different Lorentz and arc correction factor for each radiation. The intensities of fourteen arcs were measured by tracking along the zero and first layer lines with a Joyce–Loebl Mark IIIC microdensitometer using a small slit aperture. Background corrections were applied, the peak intensities were integrated along the direction of scan and the three sets of data were correlated in pairs as follows:

(i) After scaling the uncorrected data sets, a correlation factor, $R = \Sigma|I_A - I_B|/\Sigma I_A$, was calculated for each pair.
(ii) Standard rotation Lp corrections were applied, the data sets were scaled in pairs and correlation factors were again calculated.
(iii) The appropriate Lp and arc correction factors of equation (16) were applied, the data sets were scaled in pairs and correlation factors were recalculated.

The results of this analysis are reported in Table 1 in which the last three columns correspond to the three comparisons described above.

Although this limited array of data does not represent a definitive test, it is clear that the agreement between the data sets is significantly improved by the application of the proper correction factors. Moreover,

Table 1. *Correlation factors, R, between data sets corrected as described in text*

Data sets		(i)	(ii)	(iii)
A	*B*	Data uncorrected	Data Lp corrected	Data equation (16) corrected
Cu	Co	0·12	0·19	0·10
Cu	Cr	0·55	0·67	0·23
Co	Cr	0·45	0·60	0·16

since the magnitude of the correction required increases sharply for reflections at higher angles, the improved agreement achieved in the present case is particularly striking in that all of the data used were at relatively low angle.

It is interesting to note that in all cases the agreement falls off markedly when only Lp corrections are applied, even in comparison with the results for uncorrected data. Unfortunately, it is precisely this correction which is most often applied to fiber data.

It is important to recognize that the functional form of the arc correction factor corresponds to a general reduction in intensity with increasing angle and layer line height analogous to, but significantly different from, the effect of a temperature factor. Neglect of the correction in a structure analysis not only results in abnormally high temperature factors and standard deviations, but also affects the final structure. This is particularly true in the analysis of macromolecular structures displaying packing disorders.

The authors thank R. J. Fletterick for helpful discussions and acknowledge the support of the National Institutes of Health under contracts No. GM 14832-02 and No. 5 T01 GM 00334-07, as well as the Materials Science Center at Cornell University.

References

ARNOTT, S. (1965). *Polymer*, **6**, 478.
BUERGER, M. J. (1942). *X-ray Crystallography*, Ch. 8. New York: John Wiley.
BUERGER, M. J. (1960). *Crystal Structure Analysis*, Ch. 7. New York: John Wiley.
FRANKLIN, R. E. & GOSLING, R. G. (1953). *Acta Cryst.* **6**, 678.
JAMES, R. W. (1962). *The Optical Principles of the Diffraction of X-rays*, Ch. 2. Ithaca: Cornell Univ. Press.

Acta Cryst. (1970). A**26**, 124

Determination of Reduced Cells

BY A. SANTORO

Center for Radiation Research, National Bureau of Standards, Washington, D.C. 20234, *U.S.A.*

AND A. D. MIGHELL

Institute of Materials Research, National Bureau of Standards, Washington, D.C. 20234, *U.S.A.*

(*Received* 19 *March* 1969)

An analysis is given of the relation between the reduced cells defined by Niggli and the cells obtained by applying Buerger's algorithm. It is shown that in many instances a cell based on the shortest three non-coplanar translations must be transformed to obtain the reduced cell. The required transformations for all cases have been derived and are presented in this paper.

Introduction

In an important work on lattice geometry Niggli (1928) has pointed out that any crystal lattice can be represented by a positive ternary quadratic form. He has defined as *reduced cell* the cell that satisfies the conditions derived from the reduction theory of quadratic forms (Seeber, 1831; Dirichlet, 1850; Eisenstein, 1851). Such a cell provides a unique description of the lattice and is defined independently of lattice symmetry. In addition it must be primitive because one of the properties is that it is built on the shortest three non-coplanar lattice translations. Niggli has derived geometrically the reduced forms for all the Bravais lattices but he has not given any general method for converting an arbitrary primitive cell into the reduced cell.

The procedure given by Buerger (1957, 1960) and extended by Davis (1961) transforms any primitive cell into one based on the shortest three non-coplanar translations – the Buerger cell. This cell, although closely related to Niggli's reduced cell, is not unique in many cases. Some of the ambiguities associated with the Buerger cell have been discussed by Allmann (1968), especially in relation to the standard setting used by Donnay, Donnay, Cox, Kennard & King (1963) in the determinative listing of triclinic substances.

The algorithm proposed by Delaunay (1933) converts any primitive cell into a standard form involving